

Wetting Behavior of Films of New Fluorinated Styrene–Siloxane Block Copolymers

Massimo Bertolucci, Giancarlo Galli, and Emo Chiellini*

Dipartimento di Chimica e Chimica Industriale, Università di Pisa, UdR Pisa-INSTM,
Via Risorgimento 35, 56126 Pisa, Italy

Kenneth J. Wynne*

Department of Chemical Engineering, Virginia Commonwealth University, Richmond, Virginia 23284

Received December 17, 2003; Revised Manuscript Received March 15, 2004

ABSTRACT: Two new block copolymers containing dimethylsiloxane and semifluorinated styrene blocks (BSF6 and BSF8) were prepared using a polysiloxane azo-macroinitiator and corresponding semifluorinated styrene monomers StyF6 and StyF8. The thermal properties of the block copolymers were investigated by DSC, which showed the formation of a thermotropic mesophase in BSF8. This was attributed to the self-assembly of the semifluorinated side groups in microphase-separated domains of the incompatible polymer blocks. Coatings with 300 nm thicknesses had a root-mean-square roughness of 10 nm by atomic force microscopy. Using water and alcohols, wetting behavior was studied along with a model poly(dimethylsiloxane) (PDMS) network. High advancing ($\theta_{\text{adv}} = 122^\circ$) and receding ($\theta_{\text{rec}} = 82^\circ$) water contact angles were observed for BSF8. Using 2-propanol, BSF8 displayed oleophobicity ($\theta_{\text{adv}} = 64^\circ$ and $\theta_{\text{rec}} = 45^\circ$) while a reference PDMS coating was completely wetted ($\theta_{\text{adv}} = \theta_{\text{rec}} = 0^\circ$). Utilizing θ_{adv} for a series of alcohols, a fit to a modified equation of state gave a low value for BSF8 surface tension ($\gamma_{\text{SV}} = 10.5 \text{ mN/m}$). Both the wetting behavior of BSF8 and surface dynamics associated with wetting are consistent with the presence of a well-ordered, liquid crystalline fluorocarbon surface domain. In contrast, BSF6 surfaces are swollen by alcohols and display a cycle-dependent wetting behavior in water. BSF6 surfaces are thus labile to surface reorganization and/or solvent adsorption.

Introduction

The insolubility of fluorocarbons with hydrocarbons and most nonfluorinated compounds is well-known in low molar mass compounds. Perfluorinated species are insoluble or form aggregates in solution to minimize interactions with nonfluorinated compounds.^{1,2} Analogous phenomena take place when fluorocarbon and hydrocarbon segments are linked together in the same molecule by chemical bonds. The self-segregation of fluorinated segments, combined with the rigid nature of fluorocarbon chains that tend to adopt a helical conformation,^{3,4} can give rise to liquid crystalline phases.^{5–9} Ordered arrays of fluorocarbon segments exposing a uniform CF_3 order surface exhibit the lowest surface energy reported.^{10–13} Moreover, liquid crystalline organization constitutes an energetic stabilization of the surface against reconstruction induced by exposure to water or other wetting liquids.^{9,14}

Poly(dimethylsiloxane)-based materials are also long known for attractive surface properties coupled with an exceptionally low glass transition temperature, low elastic modulus, and high thermal and chemical stability.¹⁵ New macromolecular architectures combining in a single polymer the unique individual properties of both fluorinated polymers and polysiloxanes might provide interesting new materials, particularly with regard to potential for nonwetting surfaces with low surface energy. One approach to achieve such materials is the preparation of fluorinated siloxanes^{16–18} or copolymers containing fluorinated and siloxane moieties.^{12,18} Different synthetic strategies have been developed for the preparation of siloxane-based block copolymers. Siloxane copolymers have been synthesized by anionic polymerization.¹⁹ The synthesis of siloxane-containing

block or graft copolymers can also be achieved by hydrosilylation between a hydride-terminated polysiloxane and a vinyl-terminated polymer such as vinyl-terminated polystyrenes.²⁰

Another interesting approach for the synthesis of block copolymers is the use of macroinitiators. In particular, macroinitiators containing polysiloxane segments were found to be useful intermediates for the synthesis of silicone–vinyl²¹ and silicone–acrylic²² block copolymers.

To explore further the wetting characteristics in soft low surface energy polymers, our strategy focused on the study of block copolymers containing a poly(dimethylsiloxane) block and a semifluorinated polystyrene block. The surface properties of the block copolymer films were investigated by dynamic contact angle analysis with different interrogating liquids. We report our results below that indicate a surface dominated by the presence of fluorinated moieties and stabilized by a liquid crystalline mesophase of the semifluorinated side chains.

Experimental Section

a. Materials. Benzene and tetrahydrofuran were refluxed over Na/K alloy and distilled under a nitrogen atmosphere. Dichloromethane and diethyl ether were refluxed over CaH_2 and lithium aluminum hydride, respectively, and distilled under a nitrogen atmosphere. Pyridine was refluxed over KOH and distilled.

α,ω -Divinyl-terminated poly(dimethylsiloxane) ($M_w \approx 28 \text{ kDa}$), methyltris(dimethylsiloxy)silane, platinum divinyl-tetramethyldisiloxane (2.1–2.4 wt % solution in xylene), and monocarbinol-terminated poly(dimethylsiloxane) (MCR-C12, $M_n \approx 1000 \text{ Da}$, $\eta \approx 13$) were purchased from Gelest and used without further purification. All of the other commercial reagents were used without further purification.

b. Synthesis of Monomers and Polymers. The semi-fluorinated styrene monomers StyF6 and StyF8 were synthesized from 4-(chloromethyl)styrene and 1*H*,1*H*,2*H*,2*H*-perfluorooctanol and 1*H*,1*H*,2*H*,2*H*-perfluorodecanol, respectively.²³ While the former was a colorless liquid (40% yield), the latter was a waxy solid (mp 35–36 °C) (60% yield).

4,4'-Azobis(4-cyanopentanoyl chloride).²⁴ A slurry of 2.30 g (0.007 mol) of 4,4'-azobis(4-cyanopentanoic acid) in 20 mL of anhydrous benzene was chilled in an ice bath and treated with 4.47 g (0.021 mol) of phosphorus pentachloride under nitrogen. Stirring was continued for 30 min at 0 °C, and the reaction was then allowed to proceed at room temperature for 24 h. The solvent was removed under vacuum, and the solid residue was washed with anhydrous diethyl ether/*n*-hexane 1/3 v/v under nitrogen. The solid was then dissolved into anhydrous dichloromethane and precipitated in *n*-hexane. The product was recovered as a yellow-orange solid (78% yield).

IR (KBr pellet, $\bar{\nu}$, cm⁻¹): 1800 (ν C=O).

Azo-Macroinitiator (MI). To a solution of 4,4'-azobis(4-cyanopentanoyl chloride) (0.70 g, 2.2 mmol) in 50 mL of anhydrous THF were slowly added with vigorous stirring 0.4 mL of pyridine and 3.89 g (3.89 mmol of reactive units) of monocarbinol-terminated poly(dimethylsiloxane). After 24 h, the organic solution was washed with 5% HCl, 5% NaHCO₃, and water to neutrality. The solvent was then evaporated under vacuum to dryness, giving a pale yellow oil (59% yield).

IR (film on KBr, $\bar{\nu}$, cm⁻¹): 1740 (ν C=O).

¹H NMR (CDCl₃, δ , ppm): 0.1 (87H, SiCH₃), 0.5 (2H, SiCH₂), 1.6 and 1.7 (5H, SiCH₂CH₂ + CH₃), 2.5 (4H, CH₂CH₂COO), 3.4 and 3.6 (4H, CH₂OCH₂), 4.2 (2H, COOCH₂).

Poly[4-((1*H*,1*H*,2*H*,2*H*-perfluorooctyl)oxymethyl)styrene-*b*-dimethylsiloxane] (BSF6). Macroinitiator (MI, 0.11 g, 0.047 mmol of azo group), 0.50 g (1.04 mmol) of monomer StyF6, and 1.5 mL of trifluorotoluene were introduced into a glass vial, degassed by three freeze–thaw cycles, and sealed off under vacuum. The polymerization reaction was carried out at 60 °C for 48 h. The polymer was purified by precipitations into methanol from trifluorotoluene solutions (61% yield).

IR (film on KBr, $\bar{\nu}$, cm⁻¹): 3050–3020 (ν C–H aromatic), 1620–1450 (ν C=C aromatic), 1250–1030 (ν C–O–C + ν C–F), 656 (ω CF₂).

¹H NMR (CDCl₃/Cl₂CClF₂, δ , ppm): 0.1 (6H, SiCH₃), 1.4 and 1.6 (6H, CHCH₂), 2.4 (4H, CH₂CF₂), 3.7 and 4.4 (8H, CH₂OCH₂), 6.5 and 7.0 (8H, aromatic).

¹⁹F NMR (CDCl₃/CF₃CO₂H, δ , ppm): –6 (3F, CF₃), –38 (2F, CH₂CF₂), –48 to –51 (8F, 4CF₂).

Poly[4-((1*H*,1*H*,2*H*,2*H*-perfluorodecyl)oxymethyl)styrene-*b*-dimethylsiloxane] (BSF8). 0.09 g (0.038 mmol of azo group) of the macroinitiator MI, 0.49 g (0.85 mmol) of monomer StyF8, and 1.5 mL of trifluorotoluene were introduced into a glass vial, degassed by three freeze–thaw cycles, and sealed off under vacuum. The polymerization was carried out at 60 °C for 48 h. The polymer was purified by precipitations into methanol and into *n*-hexane (52% yield).

IR (film on KBr, $\bar{\nu}$, cm⁻¹): 3050–3020 (ν C–H aromatic), 1620–1450 (ν C=C aromatic), 1250–1030 (ν C–O–C + ν C–F), 656 (ω CF₂).

¹H NMR (CDCl₃/Cl₂CClF₂, δ , ppm): 0.1 (6H, SiCH₃), 1.4 and 1.6 (12H, CHCH₂), 2.4 (8H, CH₂CF₂), 3.7 and 4.4 (16H, CH₂OCH₂), 6.5 and 7.0 (16H, aromatic).

¹⁹F NMR (CDCl₃/CF₃CO₂H, δ , ppm): –6 (3F, CF₃), –38 (2F, CH₂CF₂), –48 to –52 (12F, 6CF₂).

Preparation of Cross-Linked Poly(dimethylsiloxane). α,ω -Divinyl-terminated poly(dimethylsiloxane) (5 g) was combined with 0.034 g (40 μ L) of methyltris(dimethylsiloxy)silane (SiH/vinyl ratio = 2).²⁵ The mixture was stirred by hand using a glass rod, and then platinum divinyltetramethyldisiloxane was added in order to achieve a concentration of about 30 ppm. Stirring was continued until the viscosity began to rise, at which time glass coverslips (22 \times 40 \times 0.15 mm) were dip-coated. Gelation typically occurred in 2–4 min after dip-coating, and the slides were cured upright in air at room temperature for at least 24 h.

c. Characterization. Infrared spectra were recorded with a Perkin-Elmer 1600 FT-IR spectrophotometer with 4 cm⁻¹

resolution. Samples were pressed in a KBr pellet or cast on a KBr crystal plate. ¹H (vs TMS) and ¹⁹F (vs CF₃CO₂H) NMR spectra were obtained on a Varian Gemini VRX 300 operating at 300 and 282 MHz, respectively.

Differential scanning calorimetry (DSC) measurements were performed on a Mettler DSC 30 instrument. Samples of 5–15 mg were used with 10–20 °C/min heating and cooling rates. Temperature and energy calibrations were carried out using standard samples of tin, indium, and zinc. The phase transition temperatures of the polymers were taken as corresponding to the maximum in the relevant enthalpic peak. The glass transition temperature was taken at the half devitrification of the polymer.

The polymer films for the analyses were prepared by casting a 5 wt % solution of the block copolymer in trifluorotoluene on glass coverslips and letting the solvent to evaporate slowly at room temperature. The films were annealed under vacuum at 30 °C above the *T*_g of the polymer and then slowly cooled to room temperature before the measurements. Their thickness was about 300 nm.

Dynamic contact angle (DCA) experiments were carried out by the Wilhelmy balance method using a Cahn model 312 contact angle analyzer. Purified water (~18 M Ω) was used for all samples, immersion/withdrawal rates were 100 μ m/s, and dwell times between immersion and withdrawal were 10 s, unless otherwise specified. Wetting alcohols were Aldrich products of the highest purity available. Reported contact angles are averages of several determinations. Accuracy is generally ± 1 –2°.

Tapping mode atomic force microscopy (TM-AFM) measurements were performed by imaging samples with a Digital Instruments Nanoscope IIIa with a Multimode Head. Topographic and phase contrast imaging experiments were performed. Nanoprobe cantilevers (225 μ m, Digital Instrument) were utilized. Phase contrast AFM was carried out at a set-point amplitude to cantilever free-oscillation amplitude (*A*_{sp}/*A*₀) ratios higher than 0.8, which is generally regarded as low tapping force. The root-mean-square roughness (*R*_q) was calculated by the software as

$$R_q = \sqrt{\frac{\sum_i (z_i)^2}{N}}$$

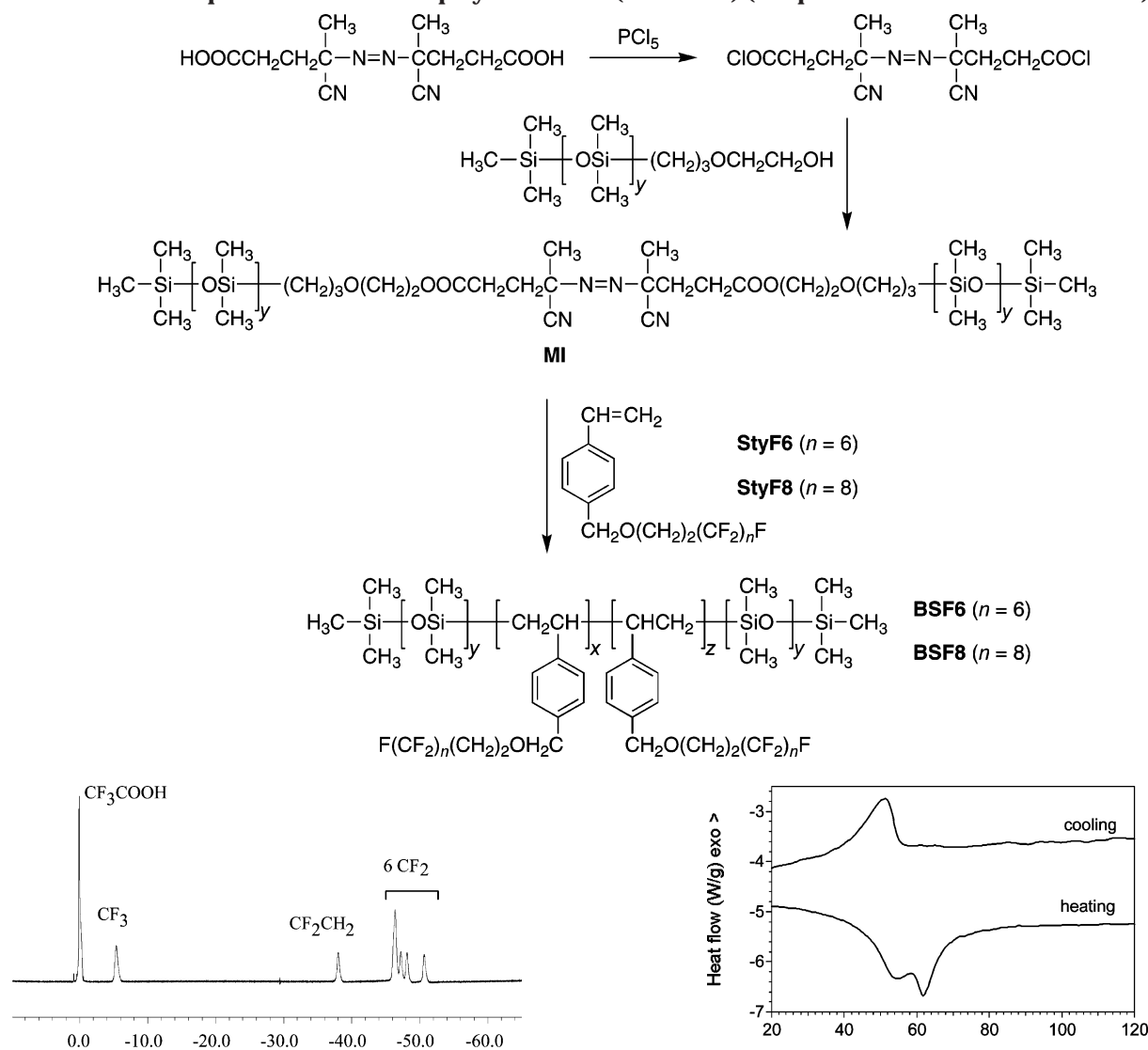
where *z*_{*i*} is the height value and *N* the number of points measured on the surface analyzed. TM-AFM measurements were carried out on the same dip-coated samples used for contact angle measurements without any additional treatment.

Results and Discussion

Preparation and Characterization. The semi-fluorinated styrenes, 4-((1*H*,1*H*,2*H*,2*H*-perfluorooctyl)oxymethyl)styrene (StyF6) and 4-((1*H*,1*H*,2*H*,2*H*-perfluorodecyl)oxymethyl)styrene (StyF8), were synthesized according to a previously reported procedure from 4-(chloromethyl)styrene and the respective semifluorinated alcohol containing a different number *n* of CF₂ groups (*n* = 6 or 8).²³

The polysiloxane azo-macroinitiator (MI) was prepared from the reaction of a monocarbinol-terminated poly(dimethylsiloxane) ($\gamma \approx 13$) with 4,4'-azobis(4-cyanopentanoyl chloride)²⁴ to give a structure comprised of one central azo group and two adjacent poly(dimethylsiloxane) blocks (Scheme 1). The block copolymers BSF6 and BSF8 were then prepared by free radical polymerization of StyF6 and StyF8, respectively, using the macroinitiator MI in trifluorotoluene solution at 60 °C (Scheme 1).

The free radical polymerization of styrene is known to terminate principally by combination.²⁶ The same preferential termination process for the fluorinated styrenes would yield principally ABA triblock copoly-

Scheme 1. Preparation of Block Copolymers BSFn (*n* = 6 or 8) (Simplified ABA Triblock Structure)**Figure 1.** ^{19}F NMR spectrum of block copolymer BSF8.**Table 1. Thermal Data for BSFn Block Copolymers**

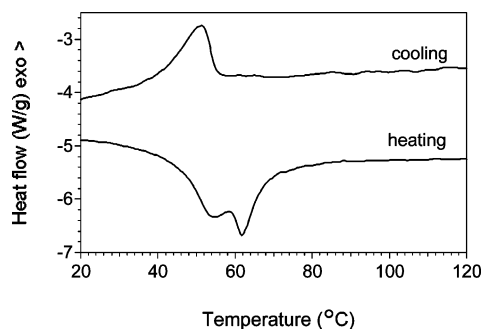
sample	<i>n</i>	<i>x</i> + <i>z</i>	<i>y</i>	<i>T_g</i> (°C) ^a	<i>T_{mes}</i> (°C) ^a
BSF6	6	56	13	14	n.d. ^b
BSF8	8	112	13	51	62

^a Glass transition and mesophase transition temperatures (by DSC at 10 °C/min heating rate). ^b Not detectable by DSC.

mers with the synthetic method used herein. Accordingly, the BSFn block copolymers are composed of a central semifluorinated polystyrene block (block B) flanked by two polysiloxane blocks (block A). Some termination by disproportionation is expected to give AB-type diblock copolymers. Therefore, the triblock copolymer structure in Scheme 1 is an approximation.

The incorporation of the fluorinated block in the block copolymers was confirmed by ^{19}F NMR (Figure 1).²⁷ The relative siloxane and styrene contents, *y* and *x* + *z*, respectively, were obtained by integration of ^1H NMR spectra (Table 1). The resonance signals centered at δ = 0.1 ppm (SiCH₃, siloxane block) and at δ = 6.5 and 7.0 ppm (aromatic, fluorinated styrene block) were clearly resolved and permitted quantitative evaluation of the block lengths.

Both copolymers showed good solubility in fluorinated solvents (trifluorotoluene and 1,1,2-trichlorotrifluoro-

**Figure 2.** First heating and cooling DSC data for block copolymer BSF8 (10 °C/min).

ethane). A clear solution was not obtained in common solvents (tetrahydrofuran, chloroform, toluene) because of aggregate formation, and therefore accurate GPC analysis was not possible in those solvents. Complete removal of any unreacted macroinitiator was ensured by repeated precipitations in *n*-hexane, which is a selective solvent for poly(dimethylsiloxane) (PDMS).

Differential Scanning Calorimetry. The semifluorinated styrene homopolymers poly(StyF6) and poly(StyF8) are known to form thermotropic, smectic mesophases.²⁸ Such mesomorphism is due to the self-assembly of the semifluorinated side chains.¹⁴ This intramolecular phase segregation results in different molecular sublayers, giving rise to a smectic mesophase. The existence of mesophase behavior shows that the siloxane and fluorinated blocks microphase separate.

The thermal behavior of the block copolymers was investigated by DSC (Figure 2 and Table 1). Only the fluorinated styrene block *T_g* is observed for both copolymers as the siloxane block *T_g* (\sim 100 °C) is below the experimental range.

In the first heating for BSF8, *T_g* is observed at 50–55 °C. In subsequent heating scans only a slight change

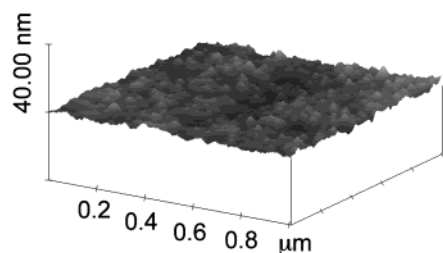


Figure 3. AFM topographic image of a BSF8 film ($R_q = 8$ nm).

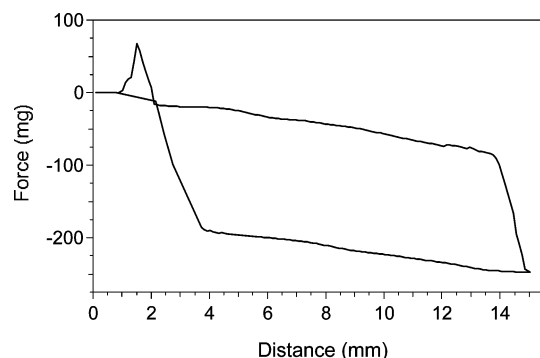


Figure 4. DCA data for BSF8 using water.

in heat capacity is observed at T_g . An endotherm for the first-order transition associated with a phase transition of a liquid crystalline mesophase is centered at $T_{mes} = 62$ °C. The reverse transition is observed about 10 °C lower during cooling. No isotropization is recorded by DSC. There is no mesophase transition detectable for BSF6; if a mesophase is present, it is of low order. These findings are consistent with previous results with fluorinated polymers, in which short semifluorinated tails favored low-order mesophases and isotropization could not be identified by DSC measurements.²⁸ Investigation by X-ray diffraction is in progress to identify the exact nature of the mesophases and to locate the isotropization temperature T_i .

Topology by AFM. One source of contact angle hysteresis is surface roughness.^{29,30} Increased surface roughness leads to higher θ_{adv} and lower θ_{rec} . Before moving to dynamic contact angle analysis, sample topology is briefly considered. Figure 3 shows a 3D height image of a typical BSF8 coating. For all block copolymer coatings the root-mean-square roughness (R_q) was lower than 10 nm. Considering recent work on silylated silicon surfaces that suggests even molecular level topological changes may effect hysteresis,^{31,32} one might be concerned about such effects on the coatings reported herein. While we do not know about the quantitative effect of this level of roughness on hysteresis, it will be seen that the differences in wetting behavior between siloxane and fluorocarbon surfaces are sufficiently great to preclude surface roughness affecting essential conclusions based on wetting behavior.

Wetting Behavior: Water. Dynamic contact angle (DCA) analysis was used for advancing (θ_{adv}) and receding (θ_{rec}) contact angles and hysteresis ($\theta_{\Delta} = \theta_{adv} - \theta_{rec}$). DCA measurements using water were taken using a large diameter (72 cm²) reservoir to avoid contamination effects that confound obtaining accurate contact angles for poly(dimethylsiloxane)-containing polymers.²⁵ The DCA force vs distance curves (fdc's) using water (Figure 4) provided $\theta_{adv} = 114^\circ$, $\theta_{rec} = 93^\circ$, and $\theta_{\Delta} = 21^\circ$ for BSF6 and $\theta_{adv} = 122^\circ$, $\theta_{rec} = 82^\circ$, and

$\theta_{\Delta} = 40^\circ$ for BSF8. High θ_{adv} and θ_{rec} demonstrate the expected hydrophobic character of the surfaces.

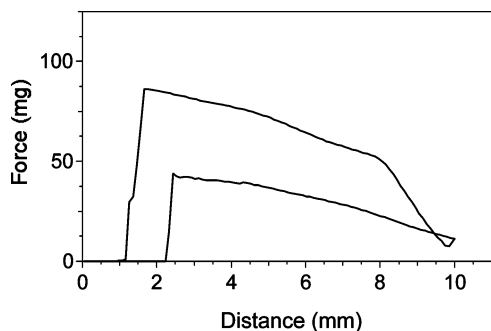
Whether hydrophobic behavior arises due to surface silicone or fluoroalkylstyrene domains (or both) cannot be decided on the basis of Wilhelmy plate data using water. That is, the observed contact angles and hysteresis fall into a range observed for either fluoropolymers or silicones. Expanding upon this point, intrinsic contact angles for model PDMS networks have been shown as $\theta_{adv} = 118^\circ$ and $\theta_{rec} = 81^\circ$.²⁵ Contact angles for polymers with semifluorinated side chains are variable depending on whether an organized surface phase exists (and if so, the size of the surface domains) and whether surface reorganization occurs, but could easily fall into the observed range. For example, Ober et al. observed high θ_{adv} (108–123°) and θ_{rec} (86–112°) for poly(styrene-*b*-semifluorinated side chain isoprene) block copolymers.^{14,33} For polymers with side chains containing $F(CF_2)_8$ high hydrophobicity was retained over time, but with $F(CF_2)_6$ side chains θ_{rec} decreases to about 50°. With a short spacer, Katano et al. observed that even perfluoro-C8 side chain containing acrylates could be “switched” from a low ($\theta_{adv} = 117^\circ$, $\theta_{rec} = 110^\circ$) to high ($\theta_{adv} = 124^\circ$, $\theta_{rec} = 58^\circ$) hysteresis state through a reversible heating/quenching process.³⁴ With an even shorter spacer, hybrid siloxane coatings cross-linked with $F(CF_2)_8(CH_2)_2Si(OC_2H_5)$ showed only a high hysteresis state ($\theta_{adv} = 135^\circ$, $\theta_{rec} = 56^\circ$).³⁵ The high hysteresis state (low θ_{rec}) was explained by the interactions of water with the acidic CH_2 protons adjacent to the CF_2 group in the fluorocarbon moiety.³⁵

While contact angles for the present block copolymers fall between the R_f -side chain limits, an increase in θ_{adv} from 114° (BSF6) to 122° (BSF8) is taken as evidence that a fluorinated phase may predominate at the surface. The observed increase is consistent with enhanced stability and order for smectic liquid crystalline phases with increasing fluorinated chain length.²⁸ However, exceptions to the trend of increased advancing contact angles with increased fluorocarbon chain length are easily found.³⁴

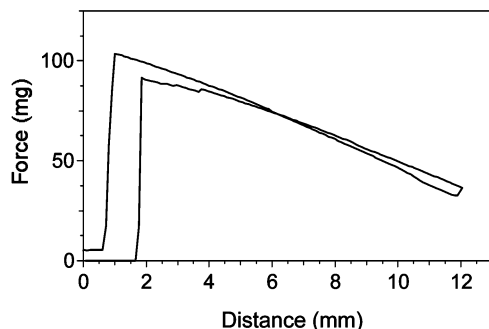
To further examine the utility of the Wilhelmy plate method in distinguishing between siloxane or fluorocarbon surfaces, other experiments with alcohols as interrogating liquids were employed.

Wetting Behavior: Alcohols. Interrogating hydroxylic liquids with surface tensions much lower than water were used to investigate the nature of the block copolymer–liquid interface (Figure 5). DCA data on the BSF8 block copolymer coatings were obtained with 1-butanol, 1-propanol, ethanol, and 2-propanol (Table 2). In addition, these solvents were used to examine a hydrosilylation-cured PDMS coating previously reported.²⁵ DCA data could not be obtained on BSF6 coatings due to swelling by these liquids.

For the BSF8 coating, a continuous increase in θ_{adv} and θ_{rec} is observed with increasing surface tension of the interrogating liquid. The same trend is seen for the PDMS coating, but the values of θ_{adv} and θ_{rec} are 20–60° lower compared to those of BSF8. Interestingly, 2-propanol perfectly wets PDMS, yielding $\theta_{adv} = \theta_{rec} = 0^\circ$. In contrast to PDMS, the corresponding values for 2-propanol/BSF8 are $\theta_{adv} = 64^\circ$ and $\theta_{rec} = 45^\circ$. The contact angle data for the alcohols clearly differentiate between PDMS and copolymer BSF8 and provide strong evidence that the BSF8 interfacial surface tension is predominantly due to a semifluorinated surface phase.



(a)



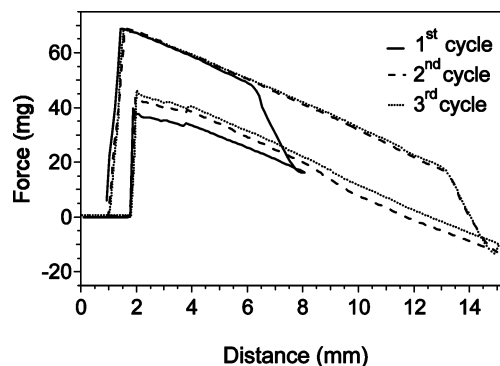
(b)

Figure 5. DCA data utilizing 2-propanol for (a) BSF8 and (b) PDMS.**Table 2. Contact Angles for PDMS and BSF8 Coatings with Water and Alcohols**

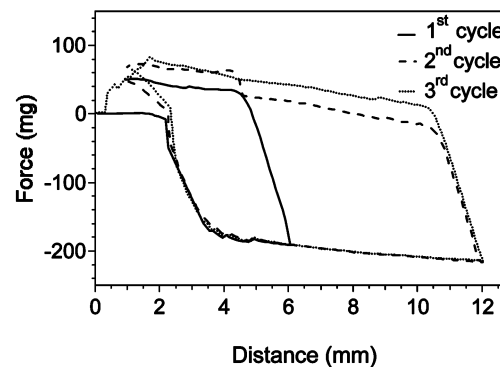
liquid	γ_{LV} (mN/m)	PDMS ($\theta_{adv}/\theta_{rec}$)	BSF8 ($\theta_{adv}/\theta_{rec}$)
water	72.6	118°/81°	122°/82°
1-butanol	25.3	42°/21°	70°/48°
1-propanol	23.6	32°/21°	68°/45°
ethanol	22.3	24°/19°	66°/45°
2-propanol	21.2	0°/0°	64°/44°

The contact angle data confirm a well-known difference between poly(dimethylsiloxane) and fluorocarbon coatings: PDMS is hydrophobic, but fluorocarbons are hydrophobic and oleophobic.

The absence of contact angle hysteresis for 2-propanol on PDMS is interesting. The deviations from linearity are attributed to variations in perimeter due to different thicknesses at the top and bottom of the coated coverslip. Contact angle hysteresis may be defined as $\gamma(\cos \theta_{rec} - \cos \theta_{adv})$, where γ is the surface tension of the wetting liquid.³⁶ The observation of zero contact angle hysteresis means that the free energy necessary to separate the liquid from the solid is equal to the energy released in contact.³⁶ However, the absolute value of the free energy may be unknown. This point is made clear by measurements that show an absence of contact angle hysteresis for flame-dried glass with either water or hexadecane. Because of strong hydrogen bonding with the surface, the heat released on water contact with glass is high but matches the energy released on dewetting. For hexadecane, which interacts only through weak van der Waals forces, the energy released on contact is small but again equal to that on dewetting. The coincidence of the advancing and receding force vs distance curves for 2-propanol/PDMS is unusual for polymers, as solvents often cause rapid reorganization or penetration of the topmost molecular layers. Thus,



(a)



(b)

Figure 6. DCA data for BSF8 in propanol, (a, dwell time after fdc-1 advancing, 5 min) and (b) water.

receding contact angles are almost always less than θ_{adv} . This is not the case for 2-propanol/Pt-cured PDMS, which implies that the energetics of wetting and dewetting are equal.

A quasi-linear relationship was found when θ_{adv} for BSF8 was plotted against γ_{LV} of the alcohols (Table 2). The contact angle data were fitted to the modified equation of state as reported by Kwok and Neumann,³⁷ giving a value of the surface tension (γ_{SV}) for BSF8 of 10.5 mN/m. This low value of γ_{SV} provides further evidence for the existence of a semifluorinated surface phase.

Surface Dynamics: BSF8. Experiments on BSF8 with 2-propanol and water were carried out to assess kinetic effects of the wetting medium (Figure 6). Using 2-propanol, the coated slide was advanced 6 mm and kept immersed for 5 min (Figure 6a).³⁸ Then the slide was reversed to the start position and advanced 12 mm, so that 6 mm of "fresh" surface was exposed.

In the first cycle θ_{adv} and θ_{rec} were 64° and 44°, respectively. In the first 6 mm of the second cycle θ_{adv} decreased to 61°, but in the second 6 mm, when fresh surface was exposed, θ_{adv} returned to the original value of 64°. No significant change was observed in θ_{rec} . In the third cycle, which interrogated surface previously exposed to 2-propanol, θ_{adv} and θ_{rec} were 59° and 43°, respectively. These are essentially the same values as those observed for the first part of the second cycle. The same result was reproduced after the slide rested in air for a few minutes. These experiments provide evidence for a reversible surface reconstruction on the time scale of the DCA experiment. Analogous results were obtained with the other alcohols.

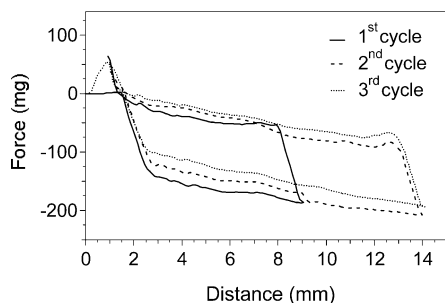


Figure 7. DCA using water for BSF6.

DCA analysis of BSF8 with the alcohols showed no evidence of liquid-phase contamination. Such contamination occurs for PDMS coatings when water is employed and is evidenced by an irreversible decrease in θ_{adv} and increase in θ_{rec} on repeating the DCA experiment.^{25,39} It is likely that the diffusion of cyclics or other species that cause this irreversible change also occurs in the alcohols, but the small quantities are apparently soluble and do not affect the measurement.

A different but similarly reversible change occurred for BSF8 in water (Figure 6b). With water, θ_{adv} remains constant (122°) for three cycles, but θ_{rec} changes reversibly from an initial 82° (fdc-r1) to 76° (fdc-r3). Importantly, no sign of water contamination is observed.

In summary, the wetting behavior of BSF8 is consistent with the presence of a well-ordered, liquid crystalline fluorocarbon surface domain. The low γ_{SV} (10.5 mN/m) attests to the dominant presence of CF_3 groups at the polymer surface. The presence of an ordered surface domain slows the kinetics of water contamination as was observed earlier for PDMS(OH)₂ cured with (fluor-organo)triethoxysilane.³⁵ The reversible changes in wetting behavior may be due to the presence of polar defects such as domain walls. Such defects would permit temporary solvent–surface interactions.

Surface Dynamics: BSF6. BSF6 showed a different behavior, with a decrease of both θ_{adv} and θ_{rec} during the second cycle (Figure 7; $\theta_{adv,1} = 114^\circ$, $\theta_{adv,2} = 110^\circ$; $\theta_{rec,1} = 93^\circ$, $\theta_{rec,2} = 91^\circ$). Further decreases are observed during the third cycle: $\theta_{adv,3} = 106^\circ$; $\theta_{rec,3} = 90^\circ$. From the observation of irregularities in the fdc's (and therefore lower data accuracy), the changes in contact angles as a function of cycle, and the swelling by alcohols noted above, it is evident that BSF6 is more labile with respect to surface reorganization and/or solvent adsorption than BSF8. The observation of a “recovery” of initial θ_{adv} in the second cycle on passing into the “fresh” surface (at 9 mm) suggests that surface reorganization accounts for the change of wetting behavior rather than water surface contamination, at least over short immersion times (about 2 min per cycle). Previous work has shown that water surface contamination leads irreversibly to a decrease in θ_{adv} but an increase in θ_{rec} .²⁵

Conclusion

Two new block copolymers BSF6 and BSF8 containing dimethylsiloxane and semifluorinated styrene blocks were prepared and characterized by NMR spectrometry and DSC. Wetting behavior with different interrogating liquids was investigated. Hydrophobic behavior in water did not distinguish between siloxane or fluoropolymer surface composition. Oleophobic behavior for BSF8 with alcohols ($\theta_{adv} = 64^\circ$ and $\theta_{rec} = 45^\circ$) was characteristic of fluorinated surfaces while a reference PDMS coating

was wetted ($\theta_{adv} = \theta_{rec} = 0^\circ$). The results for BSF8 from Wilhelmy plate DCA analysis are characteristic of fluorinated surfaces (both hydrophobic and oleophobic), in contrast to PDMS surfaces which are only hydrophobic. The higher surface stability of BSF8 compared to that of BSF6 is attributed to the thermodynamic stabilization imparted by the liquid crystalline mesophase.

Acknowledgment. The authors thank the Italian MIUR (PRIN 2001-03-4479 and 2003-03-0237) and the National Science Foundation (DMR 0207560) for financial support of the work.

References and Notes

- Höpken, J.; Möller, M.; Boileau, S. *New Polym. Mater.* **1991**, *2*, 339.
- Guittard, F.; Geribaldi, S. *J. Fluorine Chem.* **2001**, *107*, 363.
- Davidson, T.; Griffin, A. C.; Wilson, L. M.; Windle, A. H. *Macromolecules* **1995**, *28*, 354.
- Bunn, C. W.; Howells, E. R. *Nature (London)* **1954**, *174*, 549.
- Viney, C.; Russell, T. P.; Depero, L.; Twieg, R. J. *Mol. Cryst. Liq. Cryst.* **1989**, *168*, 63.
- Volkov, V. V.; Platé, N. A.; Takahara, A.; Kajiyama, T.; Amaya, M.; Murata, Y. *Polymer* **1992**, *33*, 1316.
- Wilson, L. M.; Griffin, A. C. *Macromolecules* **1994**, *27*, 128.
- Krupers, M.; Möller, M. *Macromol. Chem. Phys.* **1997**, *198*, 2163.
- Xiang, M.; Li, X.; Ober, C. K.; Char, K.; Genzer, J.; Sivanian, E.; Kramer, E. J.; Fischer, D. A. *Macromolecules* **2000**, *33*, 6106.
- Lüning, J.; Stöhr, J.; Song, K. Y.; Hawker, C. J.; Iodice, P.; Nguyen, C. V.; Yoon, D. Y. *Macromolecules* **2001**, *34*, 1128.
- Nishino, T.; Meguro, M.; Nakamae, K.; Matsushita, M.; Ueda, Y. *Langmuir* **1999**, *15*, 4321.
- Sun, F.; Castner, D. G.; Mao, G.; Wang, W.; McKeown, P.; Grainger, D. W. *J. Am. Chem. Soc.* **1996**, *118*, 1856.
- Wang, J.; Mao, G.; Ober, C. K.; Kramer, E. J. *Am. Chem. Soc., Polym. Div., Prepr.* **1997**, *38* (1), 953.
- Wang, J.; Mao, G.; Ober, C. K.; Kramer, E. J. *Macromolecules* **1997**, *30*, 1906.
- Brinker, C. J.; Scherer, G. W. *Sol–Gel Science: The Physics and Chemistry of Sol–Gel Processing*; Academic Press: Boston, 1990.
- Maxson, M. T.; Norris, A. W.; Owen, M. J. In *Modern Fluoropolymers*; Scheirs, J., Ed.; John Wiley & Sons: Chichester, UK, 1997.
- Thorpe, A. A.; Nevell, T. G.; Young, S. A.; Tsibouklis, J. *Appl. Surf. Sci.* **1998**, *136*, 99.
- Furukawa, Y.; Kotera, M. *J. Polym. Sci., Part A: Polym. Chem.* **2002**, *40*, 3120.
- Moment, A.; Miranda, R.; Hammond, P. T. *Macromol. Rapid Commun.* **1998**, *19*, 573.
- Chaumont, P.; Beinert, G.; Herz, J.; Rempp, P. *Polymer* **1981**, *22*, 663.
- Inoue, H.; Matsumoto, A.; Matsukawa, K.; Ueda, A.; Nagai, S. *J. Appl. Polym. Sci.* **1990**, *41*, 1815.
- Huan, K.; Bes, L.; Haddleton, D. M.; Khoshdel, E. *J. Polym. Sci., Part A: Polym. Chem.* **2001**, *39*, 1833.
- Andruzzi, L.; Chiellini, E.; Galli, G.; Li, X.; Kang, S. H.; Ober, C. K. *J. Mater. Chem.* **2002**, *12*, 1684.
- Smith, D. A. *Makromol. Chem.* **1967**, *103*, 301.
- Uilk, J. M.; Mera, A. E.; Fox, R. B.; Wynne, K. J. *Macromolecules* **2003**, *36*, 3689.
- Heitz, W. *Makromol. Chem., Macromol. Symp.* **1987**, *10/11*, 297.
- For assignment of ^{19}F signals see: Hazendonk, P.; Harris, R. K.; Galli, G.; Pizzanelli, S. *Phys. Chem. Chem. Phys.* **2002**, *4*, 507.
- Li, X.; Andruzzi, L.; Chiellini, E.; Galli, G.; Ober, C. K.; Hexemer, A.; Kramer, E. J.; Fischer, D. A. *Macromolecules* **2002**, *35*, 8078.
- Cassie, A. B. D. *Discuss. Faraday Soc.* **1948**, 311.
- Dettre, R. H.; Johnson, R. E. *J. Phys. Chem.* **1965**, *69*, 1507.
- Fadeev, A. Y.; McCarthy, T. J. *Langmuir* **1999**, *15*, 3759.

- (32) Chen, W.; Fadeev, A. Y.; Hsieh, M. C.; Oner, D.; Youngblood, J.; McCarthy, T. J. *Langmuir* **1999**, *15*, 3395.
- (33) Hayakawa, T.; Wang, J.; Xiang, M.; Li, X.; Ueda, M.; Ober, C. K.; Genzer, J.; Sivaniah, E.; Kramer, E. J.; Fischer, D. A. *Macromolecules* **2000**, *33*, 8012.
- (34) Katano, Y.; Tomono, H.; Nakajima, T. *Macromolecules* **1994**, *27*, 2342.
- (35) Johnston, E.; Bullock, S.; Uilk, J.; Gatenholm, P.; Wynne, K. J. *Macromolecules* **1999**, *32*, 8173.
- (36) Chaudhury, M. K.; Owen, M. J. *J. Phys. Chem.* **1993**, *97*, 5722.
- (37) Kwok, D. Y.; Neumann, A. W. *Prog. Colloid Polym. Sci.* **1998**, *109*, 170.
- (38) Ranucci, E.; Ferruti, P.; Della Volpe, C.; Migliaresi, C. *Polymer* **1994**, *32*, 5571.
- (39) We believe that the changes in contact angles occur because the surface tension of water is lowered by the formation of a coherent siloxane oil film on the surface. The nature of these species is not known as mass spectrometry experiments have not yet been successful.

MA035934X